Food Chemistry 195 (2016) 110–116

Contents lists available at ScienceDirect

Food Chemistry

journal homepage: www.elsevier.com/locate/foodchem

Potential of multispectral imaging for real-time determination of colour change and moisture distribution in carrot slices during hot air dehydration

Changhong Liu [a], Wei Liu [b], Xuzhong Lu [c], Wei Chen [a], Jianbo Yang [c], Lei Zheng [a,d,*]

[a] School of Biotechnology and Food Engineering, Hefei University of Technology, Hefei 230009, China
[b] Intelligent Control and Compute Vision Lab, Hefei University, Hefei 230601, China
[c] Rice Research Institute, Anhui Academy of Agricultural Sciences, Hefei 230031, China
[d] School of Medical Engineering, Hefei University of Technology, Hefei 230009, China

ARTICLE INFO

Article history:
Received 3 November 2014
Received in revised form 24 April 2015
Accepted 27 April 2015
Available online 6 May 2015

Keywords:
Multispectral imaging
Carrot
Moisture content
Colour change
Dehydration

ABSTRACT

Colour and moisture content are important indices in quality monitoring of dehydrating carrot slices during dehydration process. This study investigated the potential of using multispectral imaging for real-time and non-destructive determination of colour change and moisture distribution during the hot air dehydration of carrot slices. Multispectral reflectance images, ranging from 405 to 970 nm, were acquired and then calibrated based on three chemometrics models of partial least squares (PLS), least squares-support vector machines (LS-SVM), and back propagation neural network (BPNN), respectively. Compared with PLS and LS-SVM, BPNN considerably improved the prediction performance with coefficient of determination in prediction (R_P^2) = 0.991, root-mean-square error of prediction (RMSEP) = 1.482% and residual predictive deviation (RPD) = 11.378 for moisture content. It was concluded that multispectral imaging has an excellent potential for rapid, non-destructive and simultaneous determination of colour change and moisture distribution of carrot slices during dehydration.

1. Introduction

Carrot (*Daucus carota* L.) is considered one of the healthiest vegetables due to its pleasant flavour, nutritive value and great health benefits related to its antioxidant, anticancer, antianaemic, healing and sedative properties (Doymaz, 2004; Gamboa-Santos, Montilla, Soria, & Villamiel, 2012). In recent years, the consumption of carrot and its related products has increased steadily (Hiranvarachat, Devahastin, & Chiewchan, 2011). However, as with the rest of vegetables, carrot is highly seasonal and abundantly available at particular times of the year. Furthermore, carrot is a high-moisture food with moisture content of 90/100 g and wilts rapidly after harvest if it is not stored under appropriate environmental conditions, which results in poor appearance that is not acceptable to consumers (Toğrul, 2006). For extending the availability of this root, several preservation processes have been assayed. Among them, dehydration is one of the most important since it not only significantly extends vegetable shelf life and retains the nutritional quality but also diversifies the offer of foods for consumers (Prakash, Jha, & Data, 2004). Furthermore, it brings about substantial reduction in weight and volume, minimising packaging, storage and transportation costs and enables storability of the product under ambient temperatures (Baysal, Icier, Ersus, & Yıldız, 2003). Currently, dehydrated carrots are used as an ingredient in many prepared foods such as instant soups and are an excellent ingredient for developing oil-free, healthy snack foods (Lin, Durance, & Scaman, 1998). Owing to changing lifestyles, there is now a great demand for a wide variety of high quality dehydrated carrots with emphasis on freshness and convenience.

Dehydrated carrots are commonly prepared by sun drying, hot air drying, freeze drying, or vacuum microwave drying (Lin et al., 1998), and its quality, e.g., colour and moisture content, has received considerable attention from processors and consumers. The applied dehydrating conditions and pre-treatments highly influence the resulting physical, chemical, microbial, functional and organoleptic properties of the carrot products. Therefore, the improvement of carrot products quality and the rationalisation of production in many branches of industry require a permanent quality control of intermediate and finished products and continuous monitoring of technological processes. The assessment of

* Corresponding author at: School of Biotechnology and Food Engineering, Hefei University of Technology, Hefei 230009, China.
E-mail addresses: lzheng@hfut.edu.cn, lei.zheng@aliyun.com (L. Zheng).

http://dx.doi.org/10.1016/j.foodchem.2015.04.145
0308-8146/

moisture content is very important in the production of dehydrated carrots. The removal of moisture prevents the growth and reproduction of microorganisms which cause decay, and minimises many of the moisture-mediated deteriorative reactions. However, too low moisture content can badly influence food taste, and even destroy nutrition contents such as carotenoids and vitamin. In addition, the moisture content controlling has great influence on dehydrated carrots transportation and storage. Common methods for moisture analysis include oven-drying (AOAC, 1990), freeze-drying or lyophilisation (Seligman & Farber, 1971) and electronic moisture analyser (Sinija & Mishra, 2011). However, these methods are time-consuming, tedious and destructive, and not suitable for the situation where a large number of samples are required to be measured. A rapid, reliable, robust and non-destructive analytical method is needed for the prediction of moisture content in carrots during dehydration.

In addition to moisture content, the colour of the dehydrated carrots is another important quality factor, which is affected by the operation conditions. Food colour usually is the first quality parameter evaluated by consumers and is critical in the acceptance of the products. In addition, colour measurement is an objective parameter for the evaluation of quality changes during food processing, storage, and distribution. At present, colour measurements of carrots are performed using conventional colorimeter and spectral photometer after drying (Baysal et al., 2003; Rawson, Tiwari, Tuohy, O'Donnell, & Brunton, 2011; Wu, Ma, et al., 2014; Wu, Pan, et al., 2014). However, these traditional instrumental techniques are time-consuming because of the repeated measurements required to obtain a representative colour profile and to reduce the measurement error. Moreover, these instruments are designed for colour measurements on flat surfaces rather than on out-of-flatness surfaces, which are found in dehydrating carrot slices. The uncertainty of these instrumental measurements might introduce further error in analysis (Huang, Wang, Zhang, & Zhu, 2014). Furthermore, current methods for measuring moisture content and colour cannot measure the two parameters simultaneously.

Multispectral imaging is an increasingly used optical technology that integrates image with spectroscopic technique to obtain both spatial and spectral information from an object simultaneously. It has the advantages of being non-destructive, rapid, and requires no sample pre-treatment, which makes this technology directly useful for real-time applications in the field (e.g., fruit packinghouses and food processing plants) (Gowen, O'Donnell, Cullen, Downey, & Frias, 2007; Qin, Chao, Kim, Lu, & Burks, 2013). More importantly, this technique has the great potential to measure the multiple components at the same time for quality assurance. Recently, this technology has been applied as a powerful process analytical tool for non-destructive and on-line process monitoring and quality control in the food industry (Andresen, Dissing, & Løje, 2013; Kim et al., 2008; Lu & Peng, 2007; Park et al., 2007). Therefore, multispectral imaging is a promising method for industrial use since it has potential to be used as an on-line instrument for non-contact measurements of carrots on a conveyer belt during production.

To our knowledge, there is no research reported about the application of multispectral imaging technique for determining colour change and moisture distribution in carrot slices during hot air dehydration. Therefore, the overall objective of the present study was to evaluate the feasibility of using multispectral imaging technique in the spectral region of 405–970 nm for the colour change detection and moisture content prediction of carrot slices during dehydration process. The specific objectives were to: (1) determine the colour change and moisture content in carrot slices during dehydration process; (2) compare the performances of linear partial least square (PLS) and nonlinear least square-support vector machine (LS-SVM) and back propagation neural network (BPNN) analyses for the prediction accuracy of moisture content; (3) develop image processing algorithms for the visualisation of moisture content of carrot slices in all pixels within an image to form distribution maps of moisture content of carrot slices.

2. Materials and methods

2.1. Sample preparation

Two batches of fresh carrots (*D. carota* L.) were obtained from the local fruit and vegetable distribution centre of Hefei (China). Carrots with no visible damage were selected for the experiment. Carrots were properly washed in tap water to remove external impurities and cut into slices of 40 ± 2 mm diameter and 4 mm thickness. Fifty carrot slices from each batch (n = 100 slices in total) were used for analysis. The multispectral images of the carrot slices were first captured using the multispectral imaging system. Then, the sliced carrot slabs were weighed and blanched immediately in boiling water for 1 min to inactivate the enzymes responsible for quality deterioration of processed carrots (Gamboa-Santos et al., 2013). An air temperature of 60 °C was selected to simulate industrial practice and preserve the bioactivity of heat-sensitive carrot constituents. In order to obtain different levels of moisture content, carrot slices were dehydrated in a hot wind oven for seven time periods of 0, 30, 60, 120, 180, 240 and 300 min, resulting in a total of 700 samples (100 repeats for each dehydration period). For each dehydration period, each carrot sample was first scanned by the multispectral imaging system and then its reference value of moisture content was determined.

2.2. Multispectral image acquisition and analysis

The data acquisition was done using the VideometerLab equipment (Videometer A/S, Hørsholm, Denmark) which acquired the multispectral images at 19 different wavelengths ranging from 405 to 970 nm and the detailed information of the measured wavelength were 405, 435, 450, 470, 505, 525, 570, 590, 630, 645, 660, 700, 780, 850, 870, 890, 910, 940 and 970 nm. The acquisition system recorded the surface reflections with a standard monochrome charge coupled device chip, nested in a Point Grey Scorpion camera (Point Grey Research GmbH, Ludwigsburg, Germany). The carrot slice was placed inside the integrating sphere or Ulbricht sphere with a matte white coating to ensure a uniform reflection of the cast light, and thereby a uniform light in the entire sphere. At the rim of the sphere, light emitting diodes (LEDs) with narrow-band spectral radiation distribution were positioned in the pattern of side by side distributing the LEDs of each wavelength evenly across the whole perimeter to avoid shadows and specular reflections. The setup of the instrument is further described in Liu et al. (2014). The system was first calibrated radiometrically and geometrically using well-defined standard target, followed by a light setup based on the type of object to be recorded (Dissing et al., 2013). Image segmentation was performed using the VideometerLab software version 2.12.23. To remove the image background, all items except the carrot slice were removed by a Canonical Discriminant Analysis (CDA) (Cruz-Castillo et al., 1994) and segmented using a simple threshold. The mean spectra were calculated as mean values of all the pixels in carrot slice samples.

2.3. Reference measurements

The moisture content, expressed in per cent wet basis (%), was measured by the gravimetric method using the oven-drying method (AOAC, 1990). Colour values (L^*, a^* and b^* values) of carrot

slices were extracted from the image analysis and processing. L^* represents lightness, a^* represents redness or greenness while b^* represents blueness or yellowness values. Colour difference (ΔE) was used to describe the colour change in the fresh and dehydrated carrot slice samples and was calculated using the following equation (Zenoozian, Devahastin, Razavi, Shahidi, & Poreza, 2007). A larger ΔE value denoted greater colour change before and after dehydration.

$$\Delta E = \sqrt{(L_2^* - L_1^*)^2 + (a_2^* - a_1^*)^2 + (b_2^* - b_1^*)^2} \quad (1)$$

where subscripts 1 and 2 were referred to as colour components before and after dehydration, respectively.

2.4. Establishment of calibration models

In the current study, three different multivariate analysis, namely, PLS, LS-SVM and BPNN were used to establish quantitative models between moisture content and the spectral data extracted from all samples at different dehydration periods.

2.4.1. PLS

PLS is a very well-known bilinear regression method for multivariate calibration. It has been widely applied in fruits and vegetables analysis and obtained favourable results. PLS compressed a large number of variables into a few much smaller number of latent variables (LVs) that were linear combinations of the spectral data (X) and used these factors to ascertain for the analyte's concentration (Y), explaining much of the covariance of X and Y. In order to avoid the problem of over-fitting, a critical step in the algorithm is the determination of the appropriate number of LVs. This was determined by minimising the value of the prediction residual error sum of square (PRESS). In the current study, the X- and Y-variables used in the PLS models were the whole reflectance spectra and the moisture content measured by the oven-drying method, respectively.

2.4.2. LS-SVM

Support vector machine (SVM) is a learning algorithm used for classification and regression tasks proposed by Cortes and Vapnik (1995). The most valuable properties of SVM are their ability to handle large input spaces efficiently, to deal with noisy patterns and multi-modal class distributions, and their restriction on only a subset of training data in order to fit a (nonlinear) function. LS-SVM, which solves a set of linear equations instead of solving a quadratic programming problem, is an optimised version based on the standard SVM. It possesses the advantage of not only good generalisation performance as SVM, but also simpler structure and shorter optimisation time. The LS-SVM model can be expressed as:

$$y(x) = \sum_{i=1}^{n} a_i K(x, x_i) + b \quad (2)$$

where $K(x, x_i)$ is the kernel function, x_i is the input vector, α_i is Lagrange multipliers called support value and b is the bias term.

Proper kernel function and optimum kernel parameters are crucial in LS-SVM. Here, a radial basis function (RBF) with Gaussian function was used as the kernel function which handled nonlinear relationships between the spectra and target attributes and was able to reduce the computational complexity of the training procedure, giving a good performance under the general smoothness assumptions. There were just two parameters (γ, σ^2) needed for LS-SVM. The regularisation parameter γ was used to determine the trade-off between minimising the training error and model complexity. The parameter σ^2 was the bandwidth and implicitly defined the nonlinear mapping from input space to some high dimensional feature space. Leave-one-out cross-validation was used to obtain the optimum value of the parameters for the model to produce a high accuracy.

2.4.3. BPNN

One of the most popular neural network topologies is BPNN, which is used as calibration method for its supervised learning ability proved to be well suited for prediction (Mouazen, Kuang, Baerdemaeker, & Ramon, 2010). The basic structure of a BPNN was composed of three layers which are input layers, hidden layers and output layers. The input layer was used to receive information from external sources and pass this information to network for processing. The information from the input layer is processed in hidden layer and the results are sent in output layer.

The difference between the desired and calculated network output, defined as the goal error of the network, will gradually become less until it meets the desired value. The goal error of the network is calculated as:

$$E = \sum_{i=1}^{k} E_i = \frac{1}{2k} \sum_{i=1}^{k} (y_i - t_i)^2 \quad (3)$$

where k is the number of training bags, y_i is the actual output value of the ith bag and t_i is the target value of the ith bag, respectively.

An off-line training algorithm based on a gradient descent approach was used to update network weights that ensures the designed neural network converge to the desired controller output in BPNN. One cycle through all the training patterns is defined as an epoch. Before the optimal network output error is achieved for all training patterns, many epochs are required for the back propagation. The transfer function of node takes the form:

$$f(x) = \frac{1}{1 + e^{-x/Q}} \quad (4)$$

where Q is the parameter of function *Sigmoid*. As a highly non-linear mapping from input to output, the main aim of the algorithm is to find a mapping.

Leave-one-out cross-validation procedure was adopted to avoid over-fitting. Several network architectures were tested by varying the number of neurons in the hidden layer with different initial weights. The optimal parameters of the hidden nodes, the goal error and iteration times were determined by the least goal error.

2.5. Model evaluation

A total of 700 carrot slice samples were randomly divided into calibration set (75%, including 75 samples at each dehydration period) and prediction set (25%, including 25 samples at each dehydration period). To compare among different calibration models established, the coefficient of determination (R^2) in calibration (R_C^2) and prediction (R_P^2), root-mean-square error (RMSE) of calibration (RMSEC) and prediction (RMSEP) were considered. For better evaluation, the ratio between RMSEP and RMSEC was introduced, to provide information about the relationship between calibration and prediction.

Residual prediction deviation (RPD) index was determined to evaluate the robustness of the models; it was calculated as the ratio between the standard deviation of reference data and the bias-corrected RMSEP. The higher the RPD value the greater the probability of the model to predict the chemical composition in samples accurately. An RPD value range between 2.4 and 3.0 is considered poor and the models could be applied only for very rough screening, while an RPD value greater than 3.0 could be considered fair and recommended for screening purposes and good for quality control, respectively (Sinelli, Spinardi, Di Egidio, Mignani, & Casiraghi, 2008). Generally, a good model should have

high values of R_C^2, R_P^2 and RPD, low values of RMSEC and RMSEP, and a small difference between RMSEC and RMSEP.

2.6. Visualisation of moisture distribution

For detailed food analysis, it is required to visualise and analyse the distribution of spatially nonhomogeneous properties of interest in a sample, rather than their average concentration. Because each pixel in a multispectral image had a corresponding spectrum, the moisture content can be calculated at each pixel in the carrot slice sample by inputting its spectrum into the established spectral quantitative model. Then the moisture content was folded back to generate a 2-D visualised map using the positions of all corresponding pixels to visualise the moisture distribution of the carrot slice sample. All of the above computations, chemometric analyses and visualisation process were performed using the commercial software Matlab 2009 (The Mathworks Inc., Natick, MA, USA) and Origin 8.5.

3. Results and discussion

3.1. Analysis of reflectance spectra

Average reflectance spectra in the wavelength range of 405–970 nm of the examined carrot slice samples original from seven dehydration periods are shown in Fig. 1. The spectral reflectance curves of carrot slice samples at different dehydration periods were smooth and had the same trends across the whole tested wavelength region. Carotenoids are colour pigments which are responsible for imparting the characteristic orange colour to carrots. The optimal individual waveband for carotenoids estimation was identified as 470 nm (Blackburn, 1998). As shown in Fig. 1, it was clear to discover that a downward peak centred at around 470 nm, which was probably due to the presence of carotenoid in the carrot slices. In addition, a main absorption band observed between 940 and 970 nm related to O–H third stretching overtone was assigned to moisture content (Wu, He, & Feng, 2008). Furthermore, it was noticed from Fig. 1 that carrot slices with higher moisture content generally had higher reflectance spectra in the region of 405–890 nm and had lower reflectance spectra in the region of 910–970 nm. The magnitude of reflectance increased or decreased along with the increment of dehydration time. This tendency was in agreement with the real colour change and moisture content of these samples during dehydration.

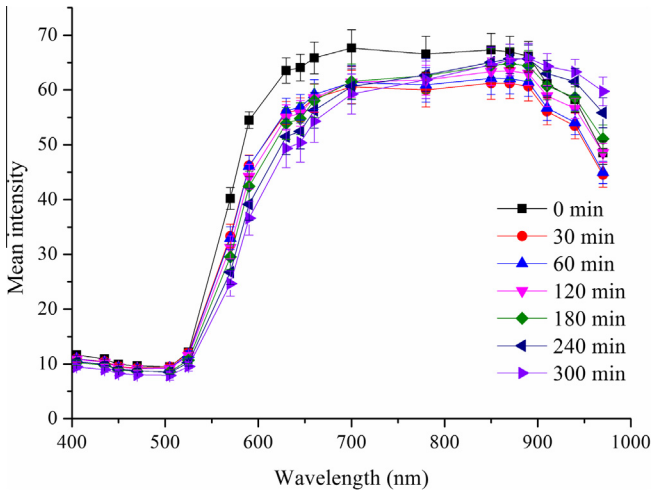

Fig. 1. Average reflection spectra of carrot slices original from seven different dehydration periods. Vertical bars represent standard deviations from one hundred measurements.

3.2. Colour change of carrot slices during dehydration

Colour change during carrot slices dehydration is due to various factors including thermal and/or oxidative destruction of carotenoids and enzymatic or non-enzymatic browning (Nahimana & Zhang, 2011). A recent paper by Løkke, Seefeldt, Skov, and Edelenbos (2013) compared CIELAB values from a spectrophotometric analysis of wild rocket leaves with those from a multispectral imaging analysis (18 wavelengths in the VIS and the NIR range of the electromagnetic spectrum) and reported that CIELAB values from the multispectral images allowed for a more detailed determination of colour compared to measurement with a spectrophotometer. Furthermore, the multispectral images enabled subtraction of background information of the sample and gave more accurate results on visual colour of wild rocket leaves. Similarly, Trinderup, Dahl, Carstensen, Jensen, and Conradsen (2013) also reported that the multispectral images (19 spectral bands, ranging from 410 to 955 nm) gave a more descriptive measure of colour and colour variance of the meat samples than the colorimeter. Based on these results, multispectral image analysis was chosen for investigating colour change of carrot slices during dehydration.

The overall colour difference (ΔE) for dehydrated carrot slices at different dehydration periods are shown in Fig. 2. The colour difference (ΔE) ranged from 4.060 to 22.762, and the mean value was 10.379, with a standard deviation of 3.886. Furthermore, due to different moisture content caused by dehydration, the carrot slices showed an appearance of colour change with a large degree of colour heterogeneity. In general, the colour of carrot slices became darker along with the progress of dehydration. Shrinkage also occurred as the carrot slice samples lost moisture content. Moreover, different visual appearance was noticed for each carrot slice indicating heterogeneous distribution of moisture content and other components in the same carrot slice. Therefore, it was necessary to utilise multispectral imaging to predict the moisture content and visualise the spatial distribution of moisture content for each carrot slice.

3.3. Spectral variation among carrot slice samples

Principal component analysis (PCA) is a common multivariate statistical modelling and analysis tool to obtain a parsimonious representation of multivariate data. In the current study, PCA was performed initially to visualise any variation among carrot

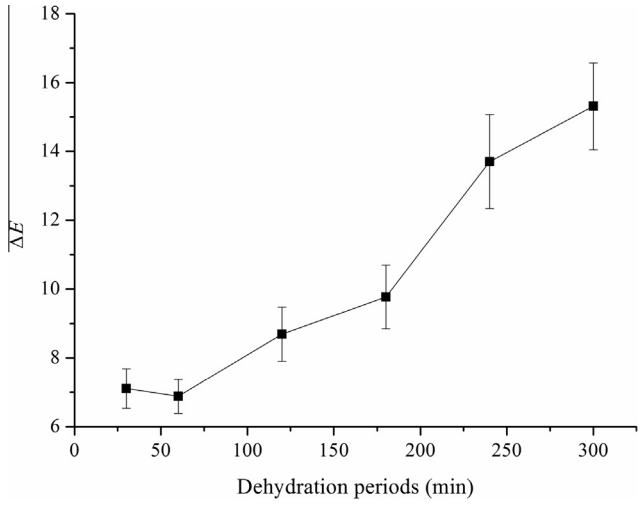

Fig. 2. Colour difference (ΔE) of carrot slices original from seven different dehydration periods. Vertical bars represent standard deviations from one hundred measurements.

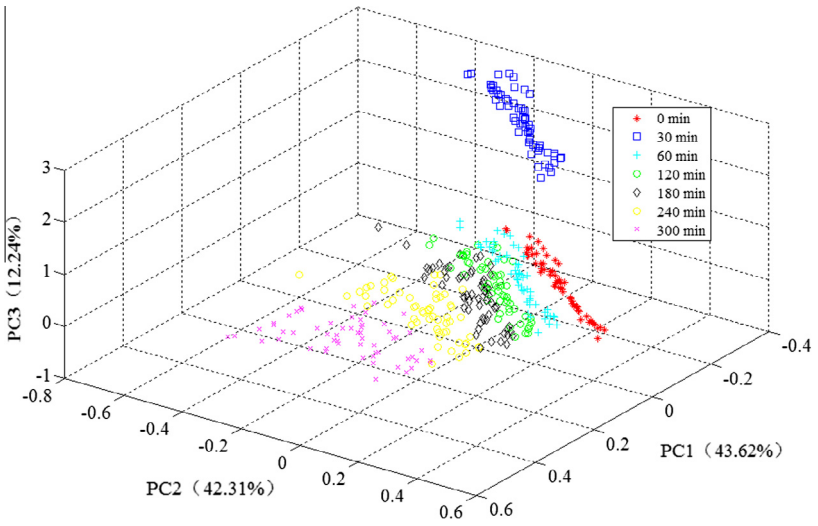

Fig. 3. Three dimensional score plot of the first three principal components conducted on the spectral data.

Table 1
Sample statistics for moisture content (%) of calibration and prediction sets.

Property	Number of samples	Minimum	Maximum	Mean	Standard deviation
Calibration set	525	15.505	92.728	74.722	18.357
Prediction set	175	21.356	91.504	74.766	17.604

slices attributed to differences in their spectral data during dehydration in principal component (PC) space. Fig. 3 shows the three dimensional score plot of the first three principal components (PCs) from the spectral data extracted from the multispectral images of all samples. The first three PCs, which account for the most spectral variations 98.17%, were used to make differentiation clearer. It was noticed that there was a better separation among samples at different dehydration periods. Furthermore, it was also observed that objects corresponding to 30 min were scored far from all the remaining periods in PC3, which was probably due to the moisture of carrot slice samples decreased faster during the first 30 min. Similar results were reported by Soria et al. (2010) and others.

3.4. Multivariate statistical analysis for moisture content

The sample statistics for moisture content of calibration and prediction sets are shown in Table 1. A wide variability in moisture content was observed as a result of the different dehydration periods: moisture content from 15.505% to 92.728%. Furthermore, structured selection using only spectral information treatment algorithms proved adequate, since the calibration and prediction sets displayed similar values for mean, standard deviation, the minimum value and the maximum value for moisture content.

The prediction performance of PLS, LS-SVM and BPNN models for the determination of moisture content in carrot slices are presented in Table 2. For PLS model, the ideal number of LVs was determined as 10 based on the lowest value of PRESS. In the stage of model development using LS-SVM with RBF kernel, the optimal combination of (γ, σ^2) was found at the value of (256, 0.0039) for moisture content prediction. For BPNN model, the optimal parameters in modelling process were set as follows after the adjustments of parameters. The number of hidden nodes, the goal error and iteration times were determined to be 0.1, 0.004 and 800 for moisture content prediction, respectively.

The selection of the best calibration model was important in spectral analysis. In the current study, the results of PLS, LS-SVM and BPNN models were compared. Compared with PLS and LS-SVM models, BPNN model had the best predictive accuracy with R_C^2 of 0.990, R_P^2 of 0.991, RMSEC of 1.344%, bias of −0.487%, RMSEP of 1.482% and RMSEP/RMSEC ratio of 1.103. According to Shenk, Workman, Westerhaus, Bums, and Ciurczak (2001), a robust model can be achieved if the corrected standard error of prediction for bias (RMSEPcorrected) does not exceed 1.30 times the RMSEC and when the bias value does not exceed 0.6 times the RMSEC. In the current study, the upper limit values were 1.103 (RMSEPcorrected/RMSEC) and 0.362 (Bias/RMSEC) in BPNN model, respectively, which indicated that the developed model was robust. Furthermore, the largest RPD of 11.378 showed that the BPNN model was considered to be adequate for process control of moisture content in carrot slices. Although the LS-SVM model had the nearly same coefficient of determination (R^2) as the BPNN model, the RMSEP was higher and RPD was lower than those in BPNN model indicating that the LS-SVM model was slightly less good for moisture content prediction. Regarding to PLS, the RMSEP was higher and R_P^2 was lower than LS-SVM and BPNN models in prediction set indicating that the model was poor. Therefore,

Table 2
Performance of PLS, LS-SVM and BPNN models for predicting moisture content (%) in carrot slices.

Calibration model	R_C^2	RMSEC	R_P^2	Bias	RMSEP	RPD	RMSEP/RMSEC
PLS	0.970	2.997	0.952	−0.537	3.420	4.930	1.141
LS-SVM	0.995	1.249	0.984	−0.985	1.925	8.757	1.542
BPNN	0.990	1.344	0.991	−0.487	1.482	11.378	1.103

R_C^2, coefficient of determination in calibration; R_P^2, coefficient of determination in prediction; RMSEC, root mean square error of calibration; RMSEP, root mean square error of prediction; RPD, residual predictive deviation.

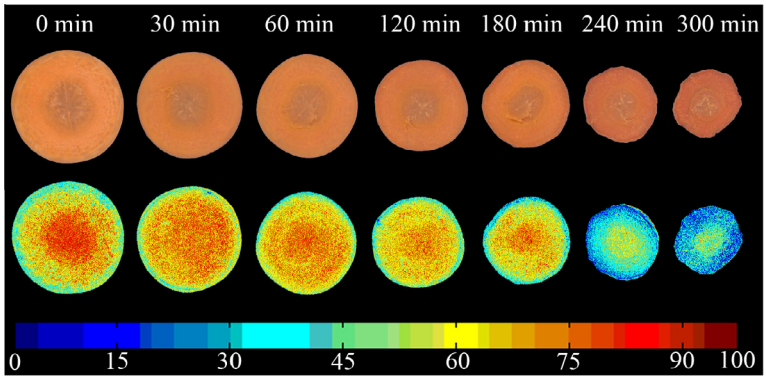

Fig. 4. Visualisation of moisture content in carrot slices at different dehydration periods.

BPNN was considered as the best way for establishing the quantitative model of moisture content in carrot slices during dehydration. The obtained model confirmed the suitability of multispectral imaging for moisture content determination in carrot slices in a non-destructive manner.

3.5. Visualisation of moisture distribution in carrot slices during dehydration

Recognising moisture distribution in a carrot slice at different dehydration periods was useful to understand the changing of moisture content in the slice during dehydration. In the current study, the selected best model was used for further visualisation of moisture content in carrot slices. An illustration of this is seen in Fig. 4, the predicted moisture content of each pixel was mapped with a linear colour scale where different moisture content from high to low were shown in different colours from red to blue (the colour bar at the bottom of Fig. 4). Because the established BPNN model had high R_P^2 of 0.991 and RPD of 11.378, and a low RMSEP of 1.482%, the resulting distribution maps were reliable.

Fig. 4 shows the final visualised images of moisture distribution of a carrot slice at seven different dehydration periods. It was observed that the intensity of moisture distribution of the carrot slice at different dehydration periods was not homogenous. This phenomenon can be explained by the different behaviour of the different tissue types, the moisture content at the xylem part of the slice was higher than that of the surrounding phloem part. Such phenomenon was much obvious for slices dehydrated after 180 min. Although many variations in moisture content were observed across the carrot slices, there was a general trend of decrease in overall moisture content from red to blue, which was a clear indication of moisture status during dehydration of carrot slices. Moreover, it was noticed that the moisture content of the surrounding part of carrot slice decreased faster than that of the centre xylem part, presumably because the surrounding part had more surface area in contact with hot air than that of the centre part. Multispectral imaging method can be more efficient for monitoring moisture content quantitatively and understanding the change of moisture distribution than using a usually much higher precision spectrometer, because the different changes of different tissue types can be compared. However, since the BPNN model in the current study, was based on the pre-processed mean spectra from the whole carrot slices, the accuracy of this pixel-wise prediction remained to be validated properly in a further study.

4. Conclusions

It has been found that multispectral imaging together with chemometrics can be successfully applied for the determination of colour change and moisture content in carrot slices during dehydration process without any preliminary sample preparation. Better prediction results for moisture content were achieved using BPNN model with R_P^2 = 0.991, RMSEP = 1.482% and RPD = 11.378, as compared with PLS and LS-SVM models. Furthermore, the simultaneous representation of both spectral and spatial data was exclusively involved in multispectral imaging techniques compared to the other spectral or optical methods. Hence, variations in moisture content in a sample could be assessed with greater details during dehydration process. The results suggest that multispectral imaging could become a promising non-destructive method for rapid and efficient inspecting the colour change and evaluating the distribution of moisture content in carrot slices during dehydration process at the processing plants.

Acknowledgements

This study is supported by the Specialized Research Fund for the Anhui Province Key Technologies Research & Development Program (1301031033), the National Key Technologies R&D Programme (2012BAD07B01), the Key Project of Anhui Provincial Educational Department (KJ2014ZD26), the Doctoral Program of Higher Education (20120111110024), the Fundamental Research Funds for the Central Universities (2012HGCX0003), the National Natural Science Foundation of China (31401544), the China Postdoctoral Science Foundation (2014M561822), and the Funds for Huangshan Professorship of Hefei University of Technology (407-037019).

References

Andresen, M. S., Dissing, B. S., & Løje, H. (2013). Quality assessment of butter cookies applying multispectral imaging. *Food Science & Nutrition, 1*, 315–323.

AOAC 950.46. (1990). *Official methods of analysis* (15th ed.). Arlington, VA: AOAC International.

Baysal, T., Icier, F., Ersus, S., & Yıldız, H. (2003). Effects of microwave and infrared drying on the quality of carrot and garlic. *European Food Research and Technology, 218*, 68–73.

Blackburn, G. A. (1998). Quantifying chlorophylls and caroteniods at leaf and canopy scales: An evaluation of some hyperspectral approaches. *Remote Sensing of Environment, 66*, 273–285.

Cortes, C., & Vapnik, V. (1995). Support vector network. *Machine Learning, 20*, 273–297.

Cruz-Castillo, J. G., Ganeshanandam, S., Mackay, B. R., Lawes, G. S., Lawoko, C. R. O., & Woolley, D. J. (1994). Applications of canonical discriminant-analysis in horticultural research. *HortScience, 29*, 1115–1119.

Dissing, B. S., Papadopoulou, O. S., Tassou, C., Ersbøll, B. K., Carstensen, J. M., Panagou, E. Z., et al. (2013). Using multispectral imaging for spoilage detection of pork meat. *Food and Bioprocess Technology, 6*, 2268–2279.

Doymaz, I. (2004). Convective air drying characteristics of thin layer carrots. *Journal of Food Engineering, 61*, 359–364.

Gamboa-Santos, J., Montilla, A., Soria, A. C., & Villamiel, M. (2012). Effects of conventional and ultrasound blanching on enzyme inactivation and carbohydrate content of carrots. *European Food Research and Technology, 234*, 1071–1079.

Gamboa-Santos, J., Soria, A. C., Pérez-Mateos, M., Carrasco, J. A., Montilla, A., & Villamiel, M. (2013). Vitamin C content and sensorial properties of dehydrated carrots blanched conventionally or by ultrasound. *Food Chemistry, 136*, 782–788.

Gowen, A. A., O'Donnell, C. P., Cullen, P. J., Downey, G., & Frias, J. M. (2007). Hyperspectral imaging – An emerging process analytical tool for food quality and safety control. *Trends in Food Science & Technology, 18*, 590–598.

Hiranvarachat, B., Devahastin, S., & Chiewchan, N. (2011). Effects of acid pretreatments on some physicochemical properties of carrot undergoing hot air drying. *Food and Bioproducts Process, 89*, 116–127.

Huang, M., Wang, Q., Zhang, M., & Zhu, Q. (2014). Prediction of color and moisture content for vegetable soybean during drying using hyperspectral imaging technology. *Journal of Food Engineering, 128*, 24–30.

Kim, M. S., Lee, K., Chao, K., Lefcourt, A. M., Jun, W., & Chan, D. E. (2008). Multispectral line-scan imaging system for simultaneous fluorescence and reflectance measurements of apples: Multitask apple inspection system. *Sensing and Instrumentation for Food Quality and Safety, 2*, 123–129.

Lin, T. M., Durance, T. D., & Scaman, C. H. (1998). Characterization of vacuum microwave, air and freeze dried carrot slices. *Food Research International, 31*, 111–117.

Liu, C., Liu, W., Lu, X., Chen, W., Yang, J., & Zheng, L. (2014). Nondestructive determination of transgenic *Bacillus thuringiensis* rice seeds (*Oryza sativa* L.) using multispectral imaging and chemometric methods. *Food Chemistry, 153*, 87–93.

Løkke, M. M., Seefeldt, H. F., Skov, T., & Edelenbos, M. (2013). Color and textural quality of packaged wild rocket measured by multispectral imaging. *Postharvest Biology and Technology, 75*, 86–95.

Lu, R., & Peng, Y. (2007). Development of a multispectral imaging prototype for real-time detection of apple fruit firmness. *Optical Engineering, 46*, 123201.

Mouazen, A. M., Kuang, B., Baerdemaeker, J. D., & Ramon, H. (2010). Comparison among principal component, partial least squares and back propagation neural network analyses for accuracy of measurement of selected soil properties with visible and near infrared spectroscopy. *Geoderma, 158*, 23–31.

Nahimana, H., & Zhang, M. S. (2011). Shrinkage and color change during microwave vacuum drying of carrot. *Drying Technology, 29*, 836–847.

Park, B., Kise, M., Lawrence, K. C., Windham, W. R., Smith, D. P., & Thai, C. N. (2007). Real-time multispectral imaging system for online poultry fecal inspection using unified modeling language. *Sensing and Instrumentation for Food Quality and Safety, 1*, 45–54.

Prakash, S., Jha, S. K., & Data, N. (2004). Performance evaluation of blanched carrots dried by three different driers. *Journal of Food Engineering, 62*, 305–313.

Qin, J., Chao, K., Kim, M. S., Lu, R., & Burks, T. F. (2013). Hyperspectral and multispectral imaging for evaluating food safety and quality. *Journal of Food Engineering, 118*, 157–171.

Rawson, A., Tiwari, B. K., Tuohy, M. G., O'Donnell, C. P., & Brunton, N. (2011). Effect of ultrasound and blanching pretreatments on polyacetylene and carotenoid content of hot air and freeze dried carrot discs. *Ultrasonics Sonochemistry, 18*, 1172–1179.

Seligman, E. B., & Farber, J. F. (1971). Freeze drying and residual moisture. *Cryobiology, 8*, 138–144.

Shenk, J. S., Workman, J. J., Westerhaus, M. O., Bums, D. A., & Ciurczak, E. W. (2001). Application of NIR spectroscopy to agricultural products. *Practical Spectroscopy Series, 27*, 419–474.

Sinelli, N., Spinardi, A., Di Egidio, V., Mignani, I., & Casiraghi, E. (2008). Evaluation of quality and nutraceutical content of blueberries (*Vaccinium corymbosum* L.) by near and mid-infrared spectroscopy. *Postharvest Biology and Technology, 50*, 31–36.

Sinija, V. R., & Mishra, H. N. (2011). FTNIR spectroscopic method for determination of moisture content in green tea granules. *Food and Bioprocess Technology, 4*, 136–141.

Soria, A. C., Corzo-Martínez, M., Montilla, A., Riera, E., Gamboa-Santos, J., & Villamiel, M. (2010). Chemical and physicochemical quality parameters in carrots dehydrated by power ultrasound. *Journal of Agricultural and Food Chemistry, 58*, 7715–7722.

Toğrul, H. (2006). Suitable drying model for infrared drying of carrot. *Journal of Food Engineering, 77*, 610–619.

Trinderup, C. H., Dahl, A. L., Carstensen, J. M., Jensen, K., & Conradsen, K. (2013). Utilization of multispectral images for meat color measurements. *Workshop on Farm Animal and Food Quality Imaging, June 17th*, 43–48.

Wu, D., He, Y., & Feng, S. (2008). Short-wave near-infrared spectroscopy analysis of major compounds in milk powder and wavelength assignment. *Analytica Chimica Acta, 610*, 232–242.

Wu, B., Ma, H., Qu, W., Wang, B., Zhang, X., Wang, P., et al. (2014a). Catalytic infrared and hot air dehydration of carrot slices. *Journal of Food Process Engineering, 37*, 111–121.

Wu, B., Pan, Z., Qu, W., Wang, B., Wang, J., & Ma, H. (2014b). Effect of simultaneous infrared dry-blanching and dehydration on quality characteristics of carrot slices. *LWT – Food Science and Technology, 57*, 90–98.

Zenoozian, M. S., Devahastin, S., Razavi, M. A., Shahidi, F., & Poreza, H. R. (2007). Use of artificial neural network and image analysis to predict physical properties of osmotically dehydrated pumpkin. *Drying Technology, 26*, 132–144.